23rd ABCM International Congress of Mechanical Engineering
December 6-11, 2015, Rio de Janeiro, RJ, Brazil

MODELING AND H_∞ CONTROL OF A CONTROL MOMENT GYROSCOPE

Bruno A. Angelico
Lab. of Automation and Control (LAC), Dept. of Telecomm. and Control, University of São Paulo, Brazil.
angelico@lac.usp.br

Diego Colón
Lab. of Automation and Control (LAC), Dept. of Telecomm. and Control, University of São Paulo, Brazil.
diego@lac.usp.br

José M. Balthazar
Department of Mechanical Engineering at Technological Institute of Aeronautics ITA, São José dos Campos, Brazil.
jmbaltha@ita.br

Abstract. *The Gyroscope is a nonlinear mechanical system that presents a very complex behavior and has several applications in engineering, from attitude and angular velocity sensors to actuator in satellites and aerospace vehicles. It can be mounted in a single gimbal configuration or in a double gimbal configuration (or freely mounted gyroscope). It also can be found in very different sizes and inertia parameters and in different combinations. In this paper, we determine the mathematical model and design a multivariable feedback control (H_∞ control) of a Control Moment Gyroscope (CMG), which is a common configuration of gyroscope found as an actuator in aerospace vehicles. The model is linearized around an arbitrary equilibrium point and parameters of stability and performance robustness are determined to aid in the design process. The controller is then implemented in a CMG experimental setup and several tests of the controller are performed and compared. Finally, direction for further research are pointed out.*

Keywords: *Gyroscope, Robust Control.*

1. INTRODUCTION

Gyroscopic systems are nonlinear mechanical devices with a large spectrum of applications in Aerospace and Naval Engineering. A Control Moment Gyroscope (CMG) is a special type of gyroscopic system which is used as actuators to aircrafts, spacecrafts and ships in order to control its attitude (orientation) in space. Normally, the CMG's rotor have constant speed, maintained by a separate control loop, and the main attitude control is designed based in this fact. A special type of CMG is the one that variation in the rotor's speed is allowed (VSCMG), which has some advantages over the traditional (fixed speed) CMG's. There are two categories of actuators for spacecraft, which are the inertial and non-inertial, as presented in Ahmed and Bernstein (2002). In the first class, we can include thrusters and magnetic actuators, and in the second class are the reaction wheels, momentum wheels and the Control Moment Gyroscopes (see for example Salatun and Bainum (1983)). Also, CMG's find applications in naval industry, as anti-rolling and anti-pitching CMG, that are devices that are used in ships to avoid the rolling and pitching oscillations due to the influence of the sea waves.

Control Moment Gyroscope (CMG) is a class of gyroscopic system in which the gyroscope is used as actuator, providing torques to an aircraft/spacecraft to control its attitude. In this case, the mechanical power involved is significantly larger than the involved in sensor systems, and the CMG are in fact devices that must store energy in larger quantities in order to generate sufficient torque for attitude control. In general, they have torque motors that act in their axis to cause rotation in different direction (of the rotor) and then produce torque in the output axis. This process in general produces a torque amplification, that must be sufficient to attitude control. CMG are more agile in attitude control systems than momentum wheels and reaction wheels (see Lappas *et al.* (2002)). Normally, CMG systems are preferred over thrusters in order to change spacecraft attitude as they do not spend nonrenewable fuel. They only need electrical power (to run the motors) that can be obtained by solar panels (see Stevenson and Schaub (2012)). Also, smaller versions of CMG systems (mini-CMG) have appeared to be used in small satellites, that cannot generate high electrical power. There are two classes of CMG: 1) single gimbal CMG (SGCMG) and 2) double gimbal CMG (DGCMG). It is also possible to assemble devices with several CMG's, in order to control attitude in the three axis. If one is intended to construct a device with only SGCMG, it will be necessary three or more of them (see Kurokawa (2007)). Commands are sent to the motors of the SGCMG in order to change its angular momentum and obtain the attitude control. A typical problem that appears in a system of SGCMG is the problem of singularity, that are different depending on the possible geometrical configurations

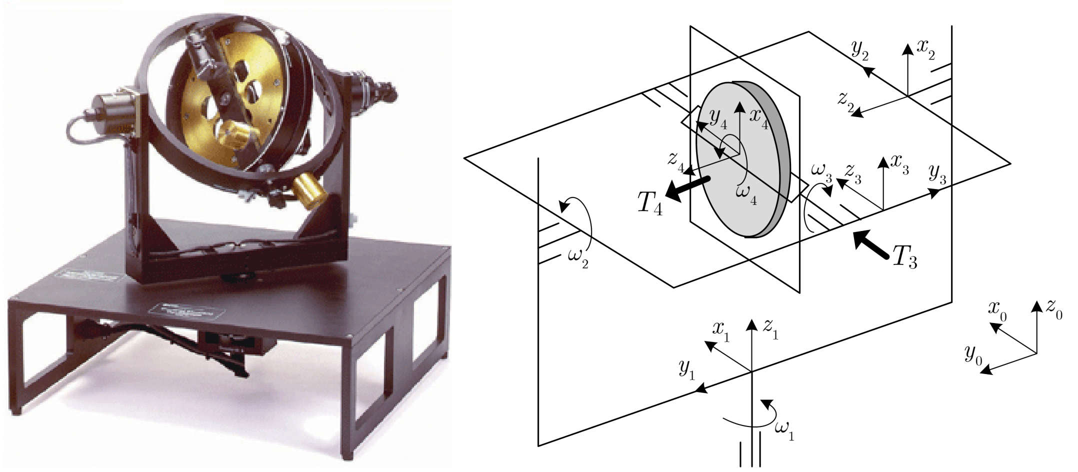

(a) Control Moment Gyroscope Parks (1999). (b) Schematic representation of the CMG.

Figure 1. Set-points and state variables.

(see Kurokawa (2007)). In this problem, there are states (gimbal angles) in which the torque output cannot assume all the possible orientations. This problem is important in order to design the attitude control laws. In general, CMG devices must maintain a constant rotor speed, and the attitude control laws are depend on this fact. In many CMG problems, on the other hand, the rotor's velocity is allowed to vary along time, as presented in Schaub *et al.* (1998). Those devices are known as Variable Speed Control Moment Gyroscopes (VSCMG), and have some advantages over fixed speed CMG, as the variable speed rotor adds an additional degree of freedom that is used to avoid the singularities (see Stevenson and Schaub (2012)). Double gimbal CMGs (or DGCMG) are more sophisticated than SGCMG as they have less problems of singularities (those only occurs in gimbal lock situation, where the inner gimbal coincides with the outer gimbal), which implies that two or more DGCMG must be used (see, for example Ahmed and Bernstein (2002)).

In this work, we present a design of a H_∞ multivariable controller for the CMG in which the rotor's angular velocity is allowed to vary (VSCMG). The gyroscope is a double gimbal CMG and robustness in the control loop is necessary in order to guarantee the stability and performance under large variations of the rotor speed. We test this control law in an experimental setup composed by the ECP© model 750 CMG (see Parks (1999)), and the control is implemented in the Real Time Windows Target from MATLAB/Simulink© in a personal computer. Other robust control strategies were evaluated in Colón *et al.* (2015). The complete system has four degrees of freedom, as shown in figures 1(a) and 1(b). The associated generalized coordinates are $\theta_1, \theta_2, \theta_3, \theta_4$ are measured by corresponding encoders, from which it can be determined also the velocities $\dot{\theta}_1, \dot{\theta}_2, \dot{\theta}_3, \dot{\theta}_4$. Also, there are two DC motors (actuators), and the control inputs to the plant are: 1) the voltage applied to the DC motor 1 that runs the disc, and 2) the voltage applied to the DC motor 2, that runs the most internal gimbal.

In section 2., some comments in the modeling process of the CMG are presented, with focus in the linearization process. In section 3, a remind of the H_∞ robust control theory is presented, as the attitude controller for the CMG must be robust in order to perform well (and remain stable) in the presence of variations in the rotor's angular velocity. In section 4., we present the important problem of controlling a VSCMG, by controlling two gimbal angles θ_1 and θ_2 by using two electric motors in the CMG, and apply the design methodology presented in section 3. In section 5, we present experimental results for the control technique presented, in the ECP© model 750 Double Gimbal CMG, and in section 6. , conclusions are suggestions for future works are presented.

2. THE MATHEMATICAL MODEL OF THE GYROSCOPE

The complete systems has four degrees of freedom, as shown in figure 1(b). The associated generalized coordinates are $\theta_1, \theta_2, \theta_3, \theta_4$ are measured by corresponding encoders[1], from which it can be determined also the velocities $\dot{\theta}_1, \dot{\theta}_2, \dot{\theta}_3, \dot{\theta}_4$. Also, there are two DC motors (actuators), and the control inputs to the plant are: 1) the voltage applied to the DC motor 1 that runs the disc, generating torque T_4, and 2) the voltage applied to the DC motor 2, that runs the gimbal 3, generating T_3. The angular position of gimbal 2 (θ_2) is mainly controlled by the reaction torque produced by changing the speed of the wheel when the voltage of the DC motor 1 changes (T_4). On the other hand, the angular position of gimbal 1 (θ_1) is mainly controlled by changing the position of gimbal 3 when the voltage of the DC motor 2 changes (T_3) (gyroscope precession).

The nonlinear dynamic equations are obtained by the Lagrange method, in which one must calculate the Lagrangian

[1] The notation of the reference frames adopted here is different (complementary) from the one presented in the manufacturer's manual.

function L, that is equal to the kinetic T energy minus the potential energy V (in this case is only gravitational). The Lagrange equations, that are presented in (1), must then be determined:

$$\frac{\mathrm{d}}{\mathrm{dt}}\frac{\partial L}{\partial \dot{\psi}_n} - \frac{\partial L}{\partial \psi_n} = T_n \tag{1}$$

where T_n is the torque in axis n, ψ_n is the generalized coordinate in axis n, $\dot{\psi}_n = \omega_n$ and $n = 1, 2, 3, 4$ (see for example Bloch (2003)). As all the center's of mass of all the bodies (rotor and gimbals) are located in the rotor's center (body D), as well as the origin of the inertial reference frame $\{0\}$, the system's Lagrangian function is equal to the kinetic energy, that is given by:

$$L = K = \sum_{n=1}^{4}\left[\frac{1}{2}\cdot m_n \cdot V_{c_n}^T \cdot V_{c_n} + \frac{1}{2}\cdot {}^n\Omega_n{}^T \cdot (I_n \cdot {}^n\Omega_n)\right] \tag{2}$$

where: 1) m_n is the mass of the rigid body n; 2) V_{c_n} is the velocity of the center of mass of the rigid body n in the inertial system $\{0\}$; 3) ${}^n\Omega_n$ is the angular velocity vector of the rigid body n in the reference frame {n}; 4) I_n is the inertia tensor of the rigid body n. As the CMG's rigid bodies do not translate, that is $V_{c_n} = 0$, the resulting Lagrangian is only:

$$L = K = \sum_{n=1}^{4}\left[\frac{1}{2}\cdot {}^n\Omega_n{}^T \cdot (I_n \cdot {}^n\Omega_n)\right] \tag{3}$$

After some manipulation, the resulting Lagrangian is given in equation:

$$\begin{aligned} L = {} & \frac{J_D}{2}\omega_4^2 + \frac{(I_C + I_D)}{2}\omega_3^2 + \frac{\left[J_B + (J_C + J_D)\cos^2(\psi_3) + (K_C + I_D)\sin^2(\psi_3)\right]}{2}\omega_2^2 + \\ & + \frac{\left\{K_A + K_B + (I_B + I_C + I_D - K_B)\sin^2(\psi_2) + \left[(K_C + I_D)\cos^2(\psi_3) + (J_C + J_D)\sin^2(\psi_3)\right]\cos^2(\psi_2)\right\}}{2}\omega_1^2 + \\ & + J_D\cos(\psi_3)\,\omega_2\omega_4 + J_D\cos(\psi_2)\sin(\psi_3)\,\omega_1\omega_4 - (I_C + I_D)\sin(\psi_2)\,\omega_1\omega_3 + \\ & + (J_C + J_D - K_C - I_D)\cos(\psi_2)\cos(\psi_3)\sin(\psi_3)\,\omega_1\omega_2 \end{aligned} \tag{4}$$

The Lagrange equations are obtained by means of a script written in MATLAB©, that delivers the nonlinear dynamic equations, as well as the linearization around the equilibrium point of operation. The equations are far too long to be presented in the paper, and the interested reader can find them in Parks (1999).

The nonlinear system model was linearized around the following equilibrium point: $\theta_1 = \theta_2 = \theta_3 = 0$, $\omega_1 = \omega_2 = \omega_3 = 0$, and $\omega_4 = \Omega$[2]. After linearizing, the complete model has the following states: $\theta_1, \theta_2, \theta_3$ and $\omega_1, \omega_2, \omega_3, \omega_4$, so the system has order seven. As the angular velocity ω_4 is constant, the state ω_4 (and its equation) is not necessary. The state θ_3 are not important in the control we are planning such that it can be excluded. Besides this fact, the system with this state is not controllable (and controllability is a necessary condition for the application of the method).

The resulting system, that is controllable and observable, has the following state, input and output vectors: $\mathbf{x} = [\theta_2\ \theta_1\ \omega_3\ \omega_2\ \omega_1]^\top$, $\mathbf{u} = [T_4\ T_3]^\top$, $\mathbf{y} = [\theta_2\ \theta_1]^\top$. The matrices of the linearized model are then:

$$A = \begin{bmatrix} 0 & 0 & 0 & 1 & 0 \\ 0 & 0 & 0 & 0 & 1 \\ 0 & 0 & 0 & 0 & \frac{J_D\Omega}{I_C+I_D} \\ 0 & 0 & 0 & 0 & 0 \\ 0 & 0 & -\frac{J_D\Omega}{I_D+K_A+K_B+K_C} & 0 & 0 \end{bmatrix}; \quad B = \begin{bmatrix} 0 & 0 \\ 0 & 0 \\ 0 & \frac{1}{I_C+I_D} \\ -\frac{1}{J_B+J_C} & 0 \\ 0 & 0 \end{bmatrix}; \quad C = \begin{bmatrix} 1 & 0 & 0 & 0 & 0 \\ 0 & 1 & 0 & 0 & 0 \end{bmatrix} \tag{5}$$

The open loop system has three eigenvalues at the origin and two pure imaginary eigenvalues which expressions are $j\omega_{\text{nutt}} = \pm j\frac{\Omega J_D}{\sqrt{(I_C+I_D)\cdot(K_A+K_B+K_C+KD)}}$. Hence, the open loop system is not asymptotically stable. The pure imaginary eigenvalues represents the nutation frequency and associated oscillatory mode that couples gimbals 3 and 1. The values of the model parameters (that can be found in Parks (1999)) are the following (all in the international system of units - SI) $K_A = 0.0667$, $I_B = 0.0119$, $J_B = 0.0178$, $K_B = 0.0297$, $I_C = 0.0092$, $J_C = 0.0229$, $K_C = 0.0221$, $I_D = 0.0148$, $J_D = 0.027$. The output sensors are incremental encoders, characterized by a certain number of counts per revolution. The encoder conversion parameters, in counts/rad, are given by (see the manual Parks (1999) for more detail): $k_{e1} = 2547\cdot 32$ (axis 1), $k_{e2} = 2547\cdot 32$ (axis 2), $k_{e3} = 3883\cdot 32$ (axis 3) and $k_{e4} = 1061\cdot 32$ (axis 4 - wheel). The amplifier dynamics is neglected, and the transformation between controllers output and torques is only the constants $k_{u3} = 9.0874\times 10^{-5}$ and $k_{u4} = 1.0772\times 10^{-5}$. The eigenvalues of the linearized system before internal feedback are $(0, 0, 0, \pm j18.8086)$.

[2] In this configuration, the 2×2 system is decoupled.

3. H_∞ ROBUST CONTROL THEORY

In this work, we will use the Loop Shaping H_∞ control, as presented in Skogestad and Postlethwaite (2005). It is an efficient method to design robust controllers and has found several practical applications. Given a multivariable plant $G(s)$, the method consists in specify the system's performance in a open loop shaping way, by augmenting the plant by using weight functions (pre and post compensators) in order to obtain an adequate format to the singular values (the performance robustness specification can also be tackled in this phase). A H_∞ synthesis problem is then solved which guarantees stability robustness. This method is essentially different from H_∞ synthesis as presented in Doyle *et al.* (1989), as in this last case, the performance specifications are given in terms of closed-loop weight functions, and a solution is obtained that theoretically optimizes the performance index (see McFarlane and Glover (1992)), but in fact an interactive procedure is conceived to successively bound the H_∞ norm until satisfactory performance is achieved (bisection method). Besides that, the loop shaping approach is valid for low and high frequencies, and not for all frequencies as in the H_∞ synthesis. On the other hand, it is more difficult to find closed-loop weight functions, and the open-loop approach of specification is more systematic. In fact, it is very similar to the LQG/LTR performance specification (see Athans (1986)).

In figure 2, we can see the block diagram for the closed-loop system, in which we are trying to obtain and multivaraible controller $K(s)$. The following equations can be easily deduced for the closed-loop system:

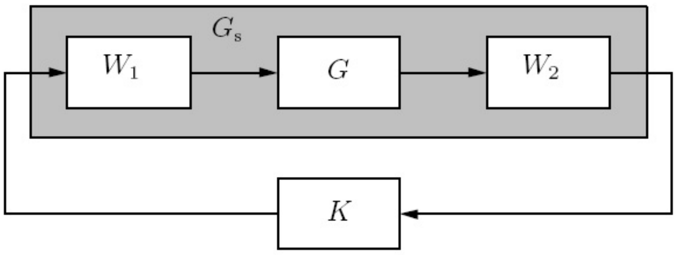

Figure 2. Closed-loop system with extended plant.

A common requirement for the closed-loop system is good disturbance and noise rejection, which can be mathematically expressed as inequalities. In the following, we present the common requirements in typical designs:

1. Good reference tracking: minimization or upper bound in $\|(I + GK)^{-1}\|_\infty$;
2. Good disturbance rejection: minimization or upper bound in $\|(I + GK)^{-1}\|_\infty$;
3. Good noise rejection: minimization or upper bound in $\|(I + GK)^{-1}GK\|_\infty$;
4. Lower control energy: minimization or upper bound in $\|K(I + GK)^{-1}\|_\infty$;

where $\|\|_\infty$ in the H_∞ norm, $(I+GK)^{-1}$ is the sensibility function and $(I+GK)^{-1}GK$ is the complementary sensibility function (see for example Doyle and Stein (1981)). In the following, we will present the design methodology of McFarlane and Glover (1992), that is known as H_∞ Loop Shaping. In this design technique, initially the nominal plant $G(s)$ must be shaped (that is, its singular values) in order to satisfy typical loop-shaping design specifications (in low and high frequencies). This plant's shaping is achieved by pre and post compensators (W_1 and W_2 respectively). The shaped plant has the expression $G_S(s) = W_1(s)G(s)W_2(s)$.

In order to obtain a controller $K(s)$ that satisfy the specification described above and guarantee stability robustness, a model of the system's uncertainties must be proposed. In figure 3, it is shown the coprime factor perturbation form of the plant $G(s) = M^{-1}(s)N(s)$, where the pair $(M, N) \in H_\infty^+$ and H_∞^+ is the space of transfer functions with no pole in the right plane. This is valid if M is square and $\det M$ is different from zero. It is supposed that there exists a pair $(V, U) \in H_\infty^+$, where $MV + NU = I$. The uncertainties are presented in figure 3, and the corresponding expression is $G_L(s) = (M_L(s) + \Delta_{M_L}(s))^{-1}(N_L(s) + \Delta_{N_L}(s))$, where $\Delta_{M_L}(s), \Delta_{N_L}(s)$ are stable but otherwise unknown transfer matrices, which represent the uncertainty in the nominal model. Also, some bounds are normally $\|\Delta_{N_L}(s)\ \Delta_{M_L}(s)\|_\infty < \epsilon$. This defines a family of possible plants, and ϵ is commonly known as *stability margin*, and generalizes, in a certain way, the concepts of gain margin and phase margin. The larger is the number, the larger is the family of possible plant. It is desirable that this stability margins be as higher as possible. In order to have stability robustness, all the plants $G_L(s)$ must be stabilized for the single controller $K(s)$. It is necessary that the closed-loop nominal system is stable, and the following H_∞ optimization problem must be solved: Find the stabilizing controller that results from the optimization problem presented in equation (6):

$$\left\| \begin{bmatrix} (I - GK)^{-1}M^{-1} \\ K(I - GK)^{-1}M^{-1} \end{bmatrix} \right\|_\infty \leq \frac{1}{\epsilon} \tag{6}$$

where K is chosen over all controllers which stabilize $G(s)$. In order to achieve the maximum ϵ, an iterative process must be used. In the case of normalized factorization, that is $\tilde{M}\tilde{M}^* + \tilde{N}\tilde{N}^* = I$, it can be proven that $\epsilon_{\text{max}} = \sqrt{(1 - \| [\, \tilde{M} \; \tilde{N} \,] \|_H^2)^{1/2}}$ and ϵ_{max} is known as the maximum stability margin, that is a theoretical limit that depends only on the model's parameters, and $\|\|_H$ is the Hankel norm (see Zhou *et al.* (1980)). When a stabilizing controller is designed such that $\epsilon = \epsilon_{\text{max}}$, one says that the an optimal controller was achieved.

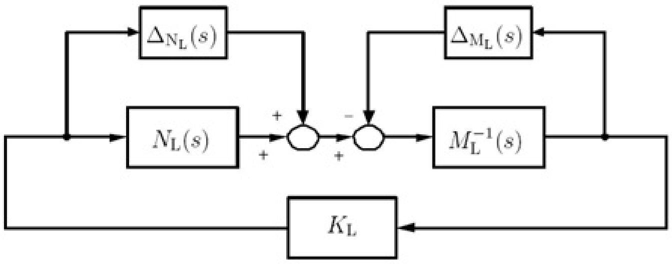

Figure 3. Transformation Between Reference Frames.

Note that it depends on the loop shaping specification, and if $\epsilon \leq \epsilon_{\text{max}} \ll 1$, this means that for this plant and specification, stability robustness is not possible.

The algorithm is the following:

1. If the number in equation (6) is much lesser than one, the loop shaping specification is not achievable and new weight should be selected.

2. else select $\epsilon \leq \epsilon_{\text{max}}$ and synthesize a stabilizing controller K which satisfy (6);

3. The final controller has the structure $W_1 K W_2$.

The loop shaping phase could also contemplate robust performance barriers, and after the synthesis of the controller $K(s)$, stability and performance robustness is guaranteed by the final controller $W_1(s)K(s)W_2(s)$. The coprime factorization must be determined in order to calculate ϵ_{max}, that amounts to solving two algebraic Riccati equations (see Skogestad and Postlethwaite (2005)). This method can produce undesirably higher order controllers, and frequently there are pole-zero cancelation in $K(s)$. A method for elimination of this poles can be used in order to reduce the controller's order.

4. CONTROL OF A VSCMG

In this section, we present the design of a closed-loop control system for a CMG based in the linearized model given in section 2.. The controller will allow the operation with variable speed in the rotor (VSCMG). In order to obtain the controller, the design methodology presented in section 3.is be used. In figure 4(a), we can see the singular values of the plant, that is the mathematical model linearized presented in equation(5). In figure 4(b), it is presented the singular values of the shaped plant, that include the specifications. The weight matrix transfer functions, that give the shape to $G_S(s)$, are: $W_1(s) = (1/s)I_{2\times 2}$ and $V_{11}(s) = 1$, $V_{12}(s) = V_{21}(s) = 0$ and $V_{22}(s) = (s - j\omega_{\text{nutt}})(s + j\omega_{\text{nutt}})/(s+10)(s+20)$, and $W_2(s) = 2W_2(0)^{-1}V(s)$. The matrix $W_1(s)$ will introduce in the controller one integrator in each channel, and $W_2(s)$ has a notch filter in the second channel, that cancel the resonant poles due to the nutation frequency ω_{nutt}.

The value calculated for ϵ_{max} is 0.1691, which is a limit imposed by the mathematical model and the specifications. The value of ϵ obtained for the design was 0.1537, that is ten percent smaller then the limit value. This is a relatively small value for the stability margin, that is due basically to the integrators in $W_1(s)$, that were added in order to attenuate disturbance. Smaller gains in low frequencies would result in better stability margins, but the system would be slower. In fact, the model deduced from the Lagrangian presented in section 2. does not include friction, that turns the system even more slow. In fact, the linearized model does not include friction, which is the reason for the undamped poles due to nutation. This friction adds stability robustness that was not considered in the H_∞ design.

Other important fact that must be stated is that the notch filter in $W_2(s)$ cancel the poles in $j\omega_{\text{nutt}}$ by means of zeros in this positions. The reader could wonder if it is a good practice, as the pole/zero cancelation is never perfect. First of all, the model's poles that are canceled are strictly in the imaginary axis and, in the worst scenario, a small oscillation would remain during the system's operation, that never grows beyond a certain limit. In fact, even this situation is an idealization, a a more precise model, that include damping, would place those poles strictly in the left half plane. So, there is no problem at all in the pole/zero cancelation of the notch filter.

In figure 5(a) it is shown the closed-loop singular values of the sensibility function, that has attenuation effect in low frequencies, which is expected in order to have good tracking properties and good disturbance rejections properties. In

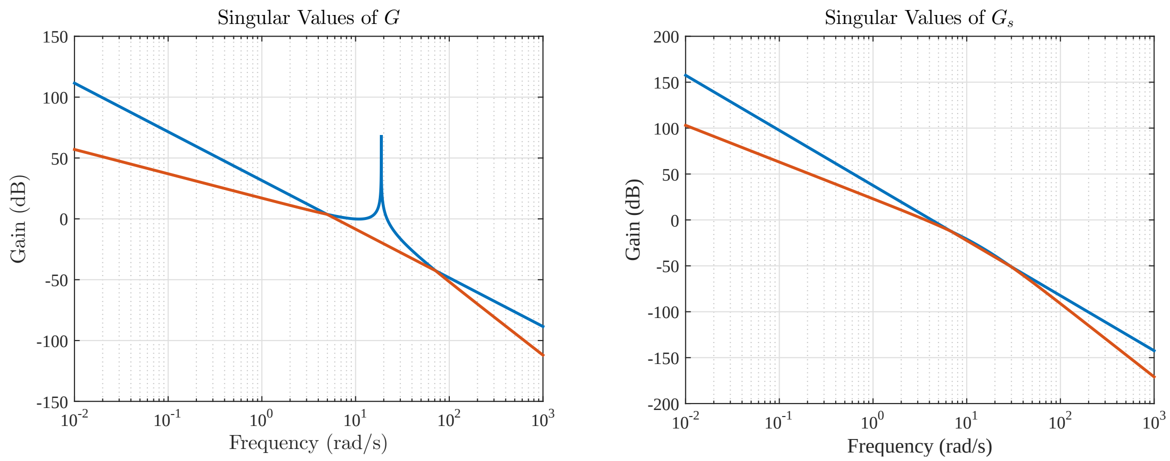

(a) Plant's Singular Values. (b) Shaped Plant' Singular Values

Figure 4. Open Loop Singular Values.

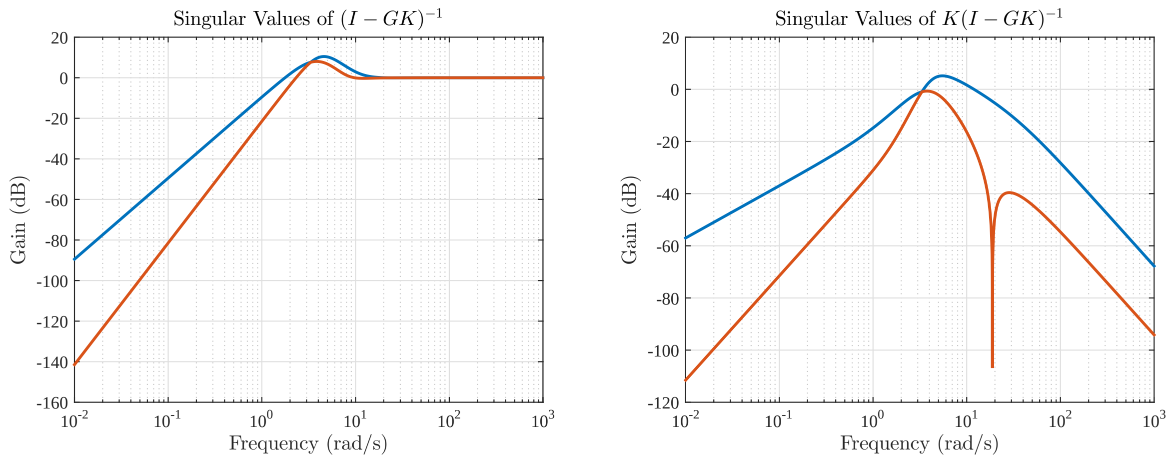

(a) Plant's Singular Values. (b) Shaped Plant' Singular Values

Figure 5. Open Loop Singular Values.

figure 5(b), we can see the singular values of the transfer function matrix $\|K(I + GK)^{-1}\|_\infty$, which indicates that the control effort is only significant in medium frequencies.

It is important to note that the linearized state space model presented in section 2. assumes that the rotor's angular velocity ω_4 is constant along the system's operation. Then, before the H_∞ control starts to running, it is necessary to control ω_4 individually until its regime velocity is achieved. We assume that this equilibrium velocity is $\Omega = 400$ rpm. This is done by another control loop, that actuates for the first 15 sec of operation. The Gyroscope has breaks that have to be activated in this initial phase in order to not have movement in the angles θ_1, θ_2. Those breaks are turned off around 10 sec, after the steady velocity $\omega_4 = \Omega$ has been achieved in order to do the proposed control. As the control of the wheel's velocity is independent of the LQG/LTR control designed, we must switch between those controllers at about 15 sec in order not to have conflicts between the loops (more details can be found in Parks (1999)).

5. EXPERIMENTAL RESULTS

In this section, we present the experimental results for the application of the multi-loop robust control technique described in section 4to the ECP© CMG presented figure 1(a) (see the manufacturer's manual Parks (1999)). In figure 6(a), we can see the reference signals for both controlled variables, which are θ_1 and θ_2 and the corresponding measured variables. We can see that the system's performance is adequate without too much overshoot. In figure 6(b), it is shown the angular velocity ω_4, that varies freely. It is expected that, after the angles achieved the desired angles, the initial controller, that maintains the angular velocity ω_4 constant, returns to activity and the H_∞ controller switches off. The control effort of the H_∞ system is presented in figure 7. Initially, motor 2 operates in saturation due to the fact that the control of ω_4 is active, and this variable have to reach the steady state angular velocity of 400 rpm (see also figure 6(b)). In 15 seconds, the H_∞ controller is activated, and a variation in θ_2 is observed. In figure 8(a), we can see the disturbance rejection capacity of the controller, and in figure 8(b), we can see the rotor's velocity in this condition.

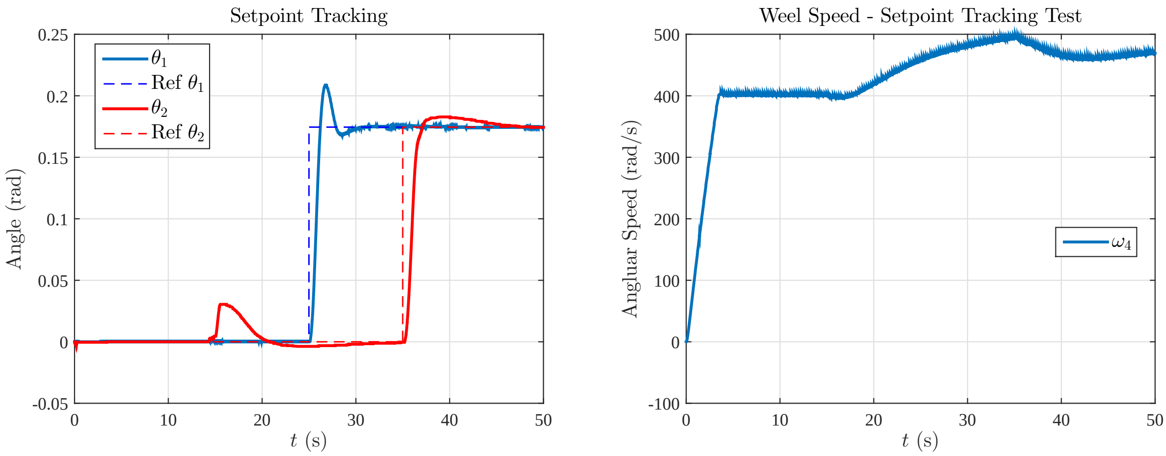

(a) Step Responses to θ_1 and θ_2.

(b) Rotor's Angular Velocity.

Figure 6. Tracking capacity of the designed H_∞ controller.

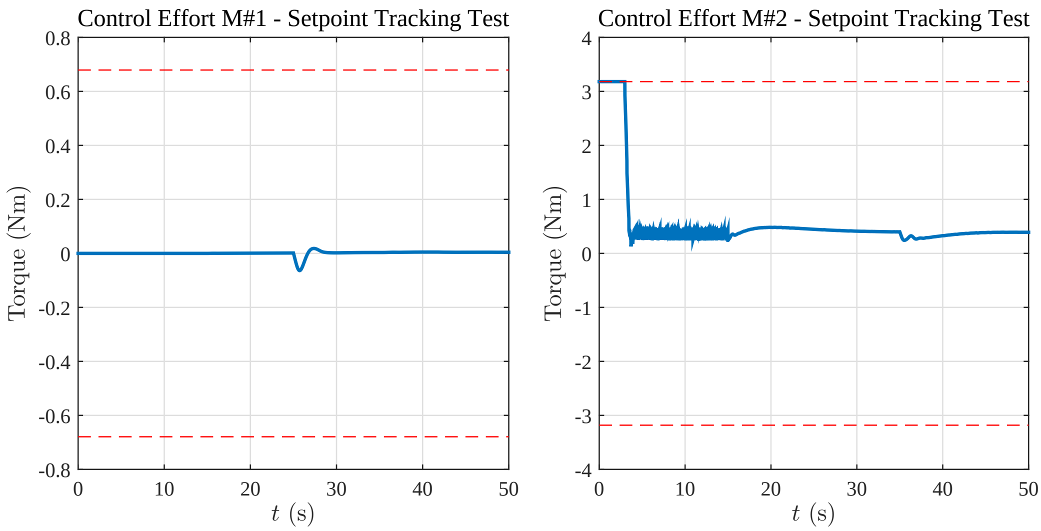

Figure 7. Control Efforts in Motors 1 and 2 - reference tracking.

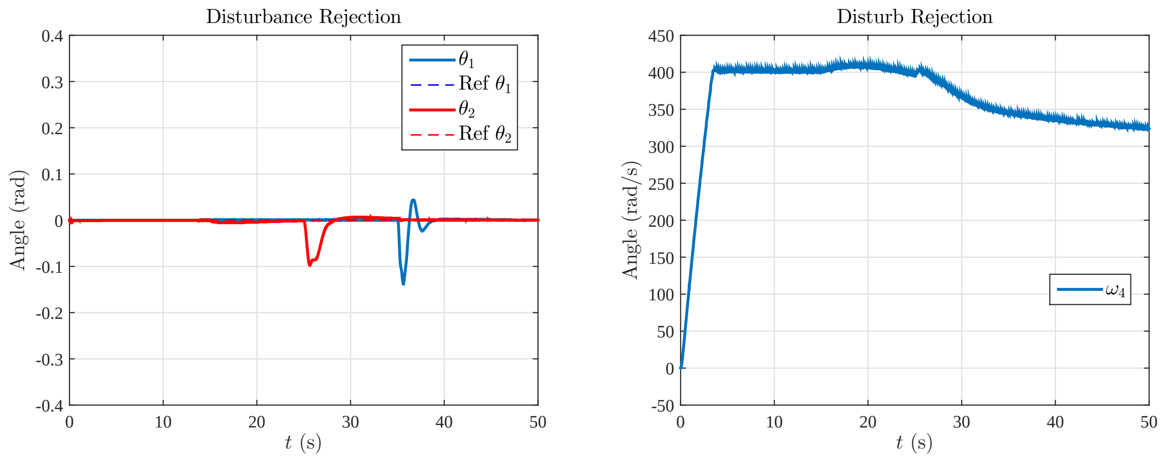

(a) Disturbance effect in θ_1 and θ_2.

(b) Corresponding Rotor's Angular Velocity.

Figure 8. Disturbance rejection capacity of the designed H_∞ controller.

6. CONCLUSIONS AND FUTURE WORK

We presented in this paper the design of a H_∞ robust controller for a Control Moment Gyroscope in which it is allowed that the rotor's angular velocity vary freely. We can see that the controller has stability robustness, as the variation in the rotor's velocity, that is only a parameter in the linearized model, do not affect significantly the system operation. The mathematical model was deduced using Lagrangian approach, but not included friction, that is predominantly of Coulomb type. The experimental results presented proves that the controller designed in robust and has reasonable performance. In future works, we intend to enhance the nonlinear mathematical model by including dry friction and shocks (see for example Colón *et al.* (2014a) and Colón *et al.* (2014c)) and test different control techniques. Also, different test for robustness could be verified, like the Polynomial Chaos approach (see for example Colón *et al.* (2014b)).

7. ACKNOWLEDGEMENTS

The first author would like to thank FAPESP for the grant 2013-25605/2.

8. REFERENCES

Ahmed, J. and Bernstein, D.S., 2002. "Adaptive control of double-gimbal control-moment gyro with unbalanced rotor". *AIAA Journal of Guidance, Control, and Dynamics*, Vol. 25, No. 1, pp. 105 – 153.

Athans, M., 1986. "A tutorial on the lqg/ltr method". In *American Control Conference, 1986*. pp. 1289–1296.

Bloch, A., 2003. *Nonholonomic Mechanics and Control*. Interdisciplinary Applied Mathematics. Springer. ISBN 9780387955353. URL `https://books.google.com.br/books?id=AhvnEzNCNaEC`.

Colón, D., Angelico, B.A., Toriumi, F.Y., Liduário, P.U.M. and Balthazar, J.M., 2015. "Geometric modeling and robust control of a gyroscopic system (to appear)". In *Proceedings of the ASME 2015 IDETC/CIE 2015*. ASME, Boston.

Colón, D., Bueno, A.M., Andrade, Y.S., Diniz, I.S. and Balthazar, J.M., 2014a. "Nonlinear ball and beam control system identification". *Applied Mechanics and Materials*, Vol. 706, pp. 69 – 80.

Colón, D., Balthazar, J.M., dos Reis, C.A., Bueno, A.M., Diniz, I.S. and de S. R. F. Rosa, S., 2014b. "Control design and robustness analysis of a ball and plate system by using polynomial chaos". *AIP Conference Proceedings*, Vol. 1637, pp. 226–234. doi:http://dx.doi.org/10.1063/1.4904583. URL `http://scitation.aip.org/content/aip/proceeding/aipcp/10.1063/1.4904583`.

Colón, D., Bueno, A.M., Diniz, I.S. and Balthazar, J.M., 2014c. "Modeling and analysis of a ball and beam system including impacts and dry friction". In *ASME 2014 International Design and Engineering Technical Conferences (IDETC/CIE 2014)*.

Doyle, J. and Stein, G., 1981. "Multivariable feedback design: Concepts for a classical/modern synthesis". *Automatic Control, IEEE Transactions on*, Vol. 26, No. 1, pp. 4–16. ISSN 0018-9286. doi:10.1109/TAC.1981.1102555.

Doyle, J., Glover, K., Khargonekar, P. and Francis, B., 1989. "State-space solutions to standard h2 and h infin; control problems". *Automatic Control, IEEE Transactions on*, Vol. 34, No. 8, pp. 831–847. ISSN 0018-9286. doi: 10.1109/9.29425.

Kurokawa, H., 2007. "Survey of theory and steering laws of single-gimbal control moment gyros". *Journal of Guidance, Control, and Dynamics*, Vol. 30, No. 5, pp. 1331–1340.

Lappas, V., Steyn, W. and Underwood, C., 2002. "Attitude control for small satellites using control moment gyros". *Acta Astronautica*, Vol. 51, No. 1âĂŞ9, pp. 101 – 111. ISSN 0094-5765.

McFarlane, D. and Glover, K., 1992. "A loop-shaping design procedure using H_∞ synthesis". *Automatic Control, IEEE Transactions on*, Vol. 37, No. 6, pp. 759–769. ISSN 0018-9286. doi:10.1109/9.256330.

Parks, T.R., 1999. *Manual For Model 750: Control Moment Gyroscope*. ECP: Educational Control Products.

Salatun, A.S. and Bainum, P.M., 1983. "Analysis of a double gimbaled reaction wheel spacecraft attitude stabilization system". *Acta Astronautica*, Vol. 10, No. 2, pp. 55 – 66. ISSN 0094-5765.

Schaub, H., R.Vadali, S. and Junkins, J.L., 1998. "Feedback control law for variable speed control moment gyroscopes". *AAS Journal of the Astronautical Sciences*, Vol. 45, No. 3, pp. 307–328.

Skogestad, S. and Postlethwaite, I., 2005. *Multivariable Feedback Control: Analysis and Design*. Multivariable Feedback Control: Analysis and Design. Wiley. ISBN 9780470011676. URL `https://books.google.com.br/books?id=3dxSAAAAMAAJ`.

Stevenson, D. and Schaub, H., 2012. "Nonlinear control analysis of a double-gimbal variable-speed control moment gyroscope". *AIAA Journal of Guidance, Control, and Dynamics*, Vol. 35, No. 3, pp. 787–793. doi:10.2514/1.56104.

Zhou, K., Doyle, J.C. and Glover, K., 1980. *Robust and Optimal Control*. Upper Saddle River, N.J.: Prentice Hall.

9. RESPONSIBILITY NOTICE

The following text, properly adapted to the number of authors, must be included in the last section of the paper:
The author(s) is (are) the only responsible for the printed material included in this paper.